MECSOL 2022 - Proceedings of the 8th International Symposium on Solid Mechanics
M.L. Bittencourt, J. Labaki, L.C.M. Vieira Jr. and E. Mesquita (Editors), Campinas SP, Brazil, October 17th to 19th, 2022

Topology optimization with connectivity constraint to separate natural frequencies of a ring structure

Heitor Nigro Lopes[1], Daniel Candeloro Cunha[1] and Renato Pavanello[1]

[1] Department of Computational Mechanics, School of Mechanical Engineering, University of Campinas, Rua Mendeleyev 200, 13083-860 Campinas, Brazil

In this work, the Virtual Flux Method (VFM) is used to ensure structural connectivity throughout the topology optimization of a ring structure. For a given operating frequency, in the high frequency domain, the objective is to obtain a structure whose natural frequencies are as far as possible from it. Without a connectivity constraint in the optimization, the structure usually degenerates, since structures with infinitesimally thin connections can potentially produce very large gaps between natural frequencies. The VFM is used to constrain the optimization problem, so that a minimal connection thickness is imposed between specified regions of the design domain. It consists in solving an auxiliary heat conduction problem, properly defined so that the flux absolute value represents a point-wise inverse measure of connectivity. This measure is used to inhibit the removal of material from regions that are essential for keeping the minimal connection thickness. Firstly, the method is illustrated for an elongated clamped-clamped beam. Then, it is applied in the optimization of a ring structure, free of mechanical restrictions. When considering the ring structure, the two regions to be kept connected overlap. This work presents how to deal with this specific issue. Results for a range of operating frequencies are presented and discussed. They show that the inclusion of the connectivity constraint through VFM successfully ensures the specified minimal connection thickness.

Keywords: Topology optimization, Connectivity constraint, Virtual flux method, Ring structure, Natural frequency separation

INTRODUCTION

Maintaining structural connectivity is a recurring challenge when optimizing natural frequencies of continuous structures. For example, the problem of maximizing the first natural frequency of a cantilever beam has the trivial solution of reducing its length, which might violate design constraints. Furthermore, maximization of higher frequencies often leads to disconnected structures (Jensen and Pedersen, 2006).

In this work, structures are optimized in order to separate their natural frequencies from a given operating frequency. As in the natural frequency maximization problems, connectivity constraints must be included to obtain proper solutions.

Introduced by Bendsøe and Kikuchi (1988), topology optimization methods are used to obtain a maximum or a minimum of a function by performing successive changes to a structure. At each iteration, a Finite Element Analysis (FEA) must be performed to evaluate how the structure should be altered in order to improve the objective function. Such optimization methods have since expanded into many different approaches, such as gradient-based methods with the Solid Isotropic Material with Penalization (SIMP) scheme (Zhou and Rozvany, 1991), or performing a succession of heuristic alterations through the Evolutionary Structural Optimization (ESO) and Bi-directional Evolutionary Structural Optimization (BESO) algorithms (Querin et al., 1998). The BESO is a discrete optimization method, that is, a single material is attributed to each element of the structure, so each element has a finite number of possible states.

Designs with optimized natural frequencies have been of interest in the field of topology optimization for a long time. Initially, Ma et al. (1994) proposed a general formulation for optimizing several different problems of natural frequencies. Xie and Steven (1996) presented a methodology for the maximization of a single or multiple natural frequencies with the ESO method, which was subsequently extended into the BESO by Yang et al. (1999).

A few problems appear in the optimization of natural frequencies. The appearance of non-physical modes is one of them. To avoid the emergence of such modes, Pedersen (2000) proposed a new interpolation scheme to be implemented with SIMP. It has been adapted for BESO by Zuo et al. (2010), allowing for a more reliable implementation of this heuristic method. Additionally, there is the mode-shifting problem, which occurs when two natural frequencies cross along the optimization process. When two or more modes coincide, their eigenvalue becomes non-differentiable, and thus, its directional derivatives must be calculated instead (Seyranian et al., 1994). Furthermore, to solve some instabilities that may arise due to the emergence of local modes and due to changes in the ordering of modes, Lopes et al. (2021)

implemented a mode-tracking algorithm that sorts modes based on the Modal Assurance Criterion (MAC) (Ewins, 2009).

When performing the optimization for natural frequency separation, results are often periodic, especially in the high-frequency domain. Olhoff et al. (2012) observed this when optimizing the natural frequency separation of Euler-Bernoulli beams. Periodic patterns have also been observed by Jensen and Pedersen (2006) in one-dimensional and two-dimensional structures modeled by a scalar wave equation.

Concerning the loss of connectivity in the optimization, several solutions have been proposed in the literature. Zhao et al. (1997) observed that adding non-structural masses aid in keeping certain areas connected. However, this changes the dynamic behavior of the system. Munk et al. (2017) proposed a connectivity filter based on the analysis of an associativity matrix. By using such filter, they could choose which elements to remove in order to avoid disconnection. Liu et al. (2015) proposed a method to avoid enclosed voids, entitled Virtual Temperature Method (VTM). Despite not being initially presented as a procedure to maintain connectivity, it has been used for that end (Pereira et al., 2022). This method utilizes the temperature of an auxiliary heat conduction problem to measure how enclosed any given void element is. Similarly, Lopes et al. (2022) introduced the Virtual Flux Method (VFM) for assuring connectivity, which uses the heat flux of an auxiliary heat conduction problem to measure connectivity.

This work employs the VFM to maintain connectivity on problems of maximization of natural frequency separation. Initially, an elongated clamped-clamped beam with two materials is optimized with and without VFM. Then, a ring structure free of mechanical constraints is optimized for different operating frequencies. Results are presented to illustrate the performance of the VFM constraint in maintaining the specified minimal connection thickness.

METHODOLOGY

Topology Optimization of Natural Frequency Separation

Considering an undamped linear dynamic system, the optimization problem to maximize the distance of the natural frequencies from a given operating frequency is stated below (Ma et al., 1994):

$$\begin{aligned} max \quad & f(x_e) = \omega_0^2 + \left[\frac{1}{N_m} \sum_{j=1}^{N_m} \frac{1}{\left(\omega_j^2 - \omega_0^2\right)^2} \right]^{-\frac{1}{2}} \\ s.t. \quad & \boldsymbol{K}\boldsymbol{\phi}_j = \omega_j^2 \boldsymbol{M}\boldsymbol{\phi}_j \\ & V^* - \sum_{e=1}^{N} V_e x_e = 0 \\ & x_e = 1 \; or \; x_{min} \end{aligned} \tag{1}$$

where ω_0 is the operating frequency of the system, N_m is the total number of evaluated modes, which must be high enough to make the process stable. If it is too high, however, computational costs can become prohibitive. The matrices $\boldsymbol{M}$ and $\boldsymbol{K}$ are, respectively, the mass and stiffness matrices, assembled and already with applied boundary conditions. The index j refer to the jth mode, being ω_j its natural frequency and $\boldsymbol{\phi}_j$ its mode shape. V^* is the imposed final volume of the system, and V_e the volume of the eth element. The discrete design variable x_e identifies whether the element is composed by material 1 ($x_e = 1$) or material 2 ($x_e = x_{min}$).

Topology optimization is a method that works by successively updating the structure based on the sensitivity of each element. To get an expression for the sensitivity value of the eth element, the objective function from Eq. 1 is differentiated with respect to x_e:

$$\alpha_e = \frac{\partial f(x_e)}{\partial x_e} = \left[\sum_{j=1}^{N_m} \frac{1}{\left(\omega_j^2 - \omega_0^2\right)^2} \right]^{-\frac{3}{2}} \sum_{j=1}^{N_m} \frac{1}{\left(\omega_j^2 - \omega_0^2\right)^3} \frac{\partial(\omega_j^2)}{\partial x_e} \tag{2}$$

where the term $\frac{\partial(\omega_j^2)}{\partial x_e}$ is the derivative of the eigenvalue. If it is a non-repeated eigenvalue, it can be directly differentiated from the Rayleigh quotient (Xie and Steven, 1996):

$$\frac{\partial(\omega_j^2)}{\partial x_e} = \boldsymbol{\phi}_j^T \left(\frac{\partial \boldsymbol{K}}{\partial x_e} - \omega_j^2 \frac{\partial \boldsymbol{M}}{\partial x_e} \right) \boldsymbol{\phi}_j \tag{3}$$

If the mode has a multiplicity greater than one, then the eigenvalue has no derivative, only directional derivatives. In that case, the following eigenproblem must be solved (Seyranian et al., 1994):

$$\left(\boldsymbol{D} - \alpha_e^{(k)} \boldsymbol{I}\right) \boldsymbol{\beta} = 0 \tag{4}$$

where $\boldsymbol{I}$ is the identity matrix, $\boldsymbol{\beta}$ is an eigenvector of the system, which represents a continuously varying eigenvector at this update direction, and $\alpha_e^{(k)}$ is the directional derivative. Each of these derivatives must be included at the summation from Eq. 2. Finally, $\boldsymbol{D}$ is a square matrix, with dimensions N_r x N_r, being N_r the multiplicity of the eigenvalue. This matrix is defined as follows:

$$\boldsymbol{D} = \begin{bmatrix} \boldsymbol{\phi}_1^T \left(\frac{\partial \boldsymbol{K}}{\partial x_e} - \omega^2 \frac{\partial \boldsymbol{M}}{\partial x_e}\right) \boldsymbol{\phi}_1 & \boldsymbol{\phi}_1^T \left(\frac{\partial \boldsymbol{K}}{\partial x_e} - \omega^2 \frac{\partial \boldsymbol{M}}{\partial x_e}\right) \boldsymbol{\phi}_2 & \cdots & \boldsymbol{\phi}_1^T \left(\frac{\partial \boldsymbol{K}}{\partial x_e} - \omega^2 \frac{\partial \boldsymbol{M}}{\partial x_e}\right) \boldsymbol{\phi}_{N_r} \\ \boldsymbol{\phi}_2^T \left(\frac{\partial \boldsymbol{K}}{\partial x_e} - \omega^2 \frac{\partial \boldsymbol{M}}{\partial x_e}\right) \boldsymbol{\phi}_1 & \boldsymbol{\phi}_2^T \left(\frac{\partial \boldsymbol{K}}{\partial x_e} - \omega^2 \frac{\partial \boldsymbol{M}}{\partial x_e}\right) \boldsymbol{\phi}_2 & \cdots & \boldsymbol{\phi}_2^T \left(\frac{\partial \boldsymbol{K}}{\partial x_e} - \omega^2 \frac{\partial \boldsymbol{M}}{\partial x_e}\right) \boldsymbol{\phi}_{N_r} \\ \vdots & \vdots & \ddots & \vdots \\ \boldsymbol{\phi}_{N_r}^T \left(\frac{\partial \boldsymbol{K}}{\partial x_e} - \omega^2 \frac{\partial \boldsymbol{M}}{\partial x_e}\right) \boldsymbol{\phi}_1 & \boldsymbol{\phi}_{N_r}^T \left(\frac{\partial \boldsymbol{K}}{\partial x_e} - \omega^2 \frac{\partial \boldsymbol{M}}{\partial x_e}\right) \boldsymbol{\phi}_2 & \cdots & \boldsymbol{\phi}_{N_r}^T \left(\frac{\partial \boldsymbol{K}}{\partial x_e} - \omega^2 \frac{\partial \boldsymbol{M}}{\partial x_e}\right) \boldsymbol{\phi}_{N_r} \end{bmatrix} \tag{5}$$

where ω is the repeated eigenvalue and $\boldsymbol{\phi}_1, \boldsymbol{\phi}_2, \cdots, \boldsymbol{\phi}_{N_r}$ are a set of $\boldsymbol{M}$-orthogonal eigenvectors.

Before performing the update, two additional procedures are done, the filtering and the historical average. Filtering is needed to avoid checkerboard patterns and to avoid mesh dependent results, it is done in two steps:

$$\alpha_n^{(nd)} = \sum_{e=1}^{M} \frac{1}{M-1} \left(1 - \frac{r_{en}}{\sum_{e=1}^{M} r_{en}}\right) \alpha_e \tag{6}$$

where $\alpha_n^{(nd)}$ are nodal sensitivities, M is the number of elements that have the node n. The value r_{en} is the distance between the center of the eth element and the nth node. If M is equal to 1, then $\alpha_n^{(nd)}$ is defined as equal to α_e.

The nodal sensitivities are averaged back into the elements as follows:

$$\alpha_e^f = \frac{\sum_{n=1}^{N_{nd}} max(0, r_m - r_{en}) \alpha_n^{(nd)}}{\sum_{n=1}^{N_{nd}} max(0, r_m - r_{en})} \tag{7}$$

where N_{nd} is the total number of nodes. The parameter r_m is the filter radius.

The second procedure is the historical average, used to stabilize the iterative optimization process. It is done as follows:

$$\alpha_e^{h(k)} = \frac{\alpha_e^{f(k)} + \alpha_e^{h(k-1)}}{2} \tag{8}$$

where $\alpha_e^{h(k)}$ is the sensitivity with historical average for the current iteration, $\alpha_e^{f(k)}$ is the filtered sensitivity obtained in this iteration, and $\alpha_e^{h(k-1)}$ represents the averaged sensitivity from the previous iteration. At the first iteration, $\alpha_e^{h(k-1)}$ is set to zero.

With the final sensitivities, the structure is updated by altering certain solid elements to void and some void to solid. The number of elements to be changed is based on two parameters. The first one is the Evolutionary Rate (ER), which establishes the target volume of the current iteration. The second one is the maximum Addition Ratio (AR_{max}), which limits the number of void elements that can become solid at any given iteration.

The considered stop criterion is based on the relative variation of the objective function in the last $2P$ iterations. After V^* has been reached, the variation ε is computed in each iteration as follows:

$$\varepsilon^{(k)} = \frac{\left| \sum_{q=k-2P+1}^{k-P} f(\boldsymbol{x}^{(q)}) - \sum_{q=k-P+1}^{k} f(\boldsymbol{x}^{(q)}) \right|}{\sum_{q=k-P+1}^{k} f(\boldsymbol{x}^{(q)})} \tag{9}$$

The procedure stops when ε becomes smaller than a specified tolerance value, τ.

Virtual Flux Method (VFM)

Without the inclusion of connectivity constraints, the separation of natural frequencies through topology optimization may lead to disconnected structures. This happens when structures with infinitesimally thin connections between its components have high performance values according to the specified objective function. These are undesirable, improper solutions, in terms of practicality and manufacturability, which are not taken into account in the objective function.

To deal with this issue, the Virtual Flux Method (VFM) (Lopes et al., 2022) is used to ensure a minimal connection area throughout the optimization procedure. This method provides a quantitative measure of the importance of each element in keeping two given regions connected.

In order to compute such measure in each iteration of the optimization procedure, a virtual steady-state heat conduction problem is considered. A unitary thermal conductivity is attributed to the solid elements of the current topology, and a nearly zero conductivity is attributed to the void ones. Then, the following heat problem is solved:

$$\begin{array}{lll} \nabla \cdot (k(\boldsymbol{r}) \nabla T(\boldsymbol{r})) = -q_V(\boldsymbol{r}) & , & for\ \boldsymbol{r} \in \Omega \\ \nabla T(\boldsymbol{r}) \cdot \boldsymbol{n}(\boldsymbol{r}) = 0 & , & for\ \boldsymbol{r} \in \partial\Omega \\ T(\boldsymbol{r}) = 0 & , & for\ \boldsymbol{r} \in \{\boldsymbol{r_0}\} \end{array} \tag{10}$$

where Ω is the design domain; $\boldsymbol{r_0}$ can be any point of Ω (the condition over $\{\boldsymbol{r_0}\}$ is defined so that the problem is well-posed); and q_V is the volumetric heat source.

Let Γ_{in} and Γ_{out} be the regions of the design domain which must be kept connected, then, q_V is defined so that $1\,W$ enters the system through Γ_{in} and the same $1\,W$ exits the system through Γ_{out}. The volumetric heat source is zero in $\Omega/(\Gamma_{in} \cup \Gamma_{out})$.

After solving the virtual problem and obtaining the temperature vector, the corresponding heat flux can be computed for any point of the solid structure. Thin connections are expected to have high flux values, while thick connections are expected to have low flux values. Thus, the mean flux norm of each solid element is taken as a measure of its importance in keeping Γ_{in} and Γ_{out} connected.

Since solid elements with high mean flux norm values are critical, they must not be turned into void elements in the current iteration of the optimization algorithm. For the BESO method, this is imposed through the following alteration of the final sensitivity value of each solid element:

$$\alpha_e^c = \alpha_e^h + c(q_e)\,[\max(\boldsymbol{\alpha}^h) - \alpha_e^h] \tag{11}$$

where q_e is the mean flux norm of the e-th element, and $c(\cdot)$ is an activation function.

In this work, a linear activation has been considered:

$$c(q_e) = \begin{cases} 0 & , \quad if\ q_e < q_{act} \\ \frac{q_e - q_{act}}{q_{lim} - q_{act}} & , \quad if\ q_e \in [q_{act}, q_{lim}] \\ 1 & , \quad if\ q_e > q_{lim} \end{cases} \tag{12}$$

where, for a given limit value for the connection area A_{lim} and "activation area" $A_{act} \geq A_{lim}$, $q_{act} = \frac{1}{A_{act}}$ and $q_{lim} = \frac{1}{A_{lim}}$. Any element such that $q_e \geq q_{act}$ is partially constrained and any element such that $q_e \geq q_{lim}$ is completely constrained. The partial constraints are applied in order to inhibit oscillating behaviors.

To enable void elements to be turned into solid ones in critical regions, the filtering and historical average procedures for void elements are only performed after the VFM alteration.

Finally, the optimization problem with an imposed connectivity constraint can be stated as:

$$\begin{array}{ll} max & f(x_e) = \omega_0^2 + \left[\frac{1}{N_m} \sum_{j=1}^{N_m} \frac{1}{\left(\omega_j^2 - \omega_0^2\right)^2} \right]^{-\frac{1}{2}} \\ s.t. & \boldsymbol{K}\boldsymbol{\phi}_j = \omega_j^2 \boldsymbol{M}\boldsymbol{\phi}_j \\ & V^* - \sum_{e=1}^{N} V_e x_e = 0 \\ & q_e \leq q_{lim} \\ & x_e = 1\ or\ x_{min} \end{array} \tag{13}$$

Algorithm 1 shows how this problem can be solved through the BESO method coupled with the VFM.

Algorithm 1: BESO topology optimization algorithm with VFM

Input: Define parameters: ER, AR_{max}, V^*, r_m, τ, P, Γ_{in}, Γ_{out}, A_{act}, A_{lim}

k = 0
Define initial topology
Perform FEA for the real system
Compute objective function
$\varepsilon^{(k)} = \tau + 1$
while $\varepsilon^{(k)} > \tau$ ***or*** $V^{(k)} \neq V^*$ **do**
  Compute the raw sensitivity values (Eq. 2)
  Filter the sensitivity values for elements with $x_e = 1$ according to r_m (Eqs. 6 and 7)
  Perform historical average for elements with $x_e = 1$ (Eq. 8)
  Perform FEA for the virtual system according to Γ_{in} and Γ_{out}
  Compute activation values according to A_{act} and A_{lim} (Eq. 12)
  Alter the sensitivity vector according to activation values (Eq. 11)
  Filter the sensitivity values for elements with $x_e = x_{min}$ according to r_m
  Perform historical average for elements with $x_e = x_{min}$
  Sort elements by their final sensitivity values
  k = k + 1
  Define $V^{(k)}$ according to $V^{(k-1)}$, V^* and ER
  Update topology according to $V^{(k)}$ and AR_{max}
  Perform FEA for the real system
  Compute objective function
  if $k \geq 2P - 1$ **then**
    Compute $\varepsilon^{(k)}$ (Eq. 9)
  else
    $\varepsilon^{(k)} = \tau + 1$
  end
end
Output: Optimized topology

RESULTS AND DISCUSSION

Clamped-clamped Beam

Initially, a clamped-clamped elongated beam is considered, as illustrated in Figure 1. The dimensions of the beam are $L_x = 2000$ mm and $L_y = 100$ mm. The VFM is used to impose that the extremities of the beam are kept connected. In order to do so, Γ_{in} is set on the left edge of the rectangular domain, and Γ_{out} is set on the right edge. Since this is a bidimensional structure, VFM constraint imposes a minimal thickness value instead of a minimal area value, so A_{act} and A_{lim} correspond to length values.

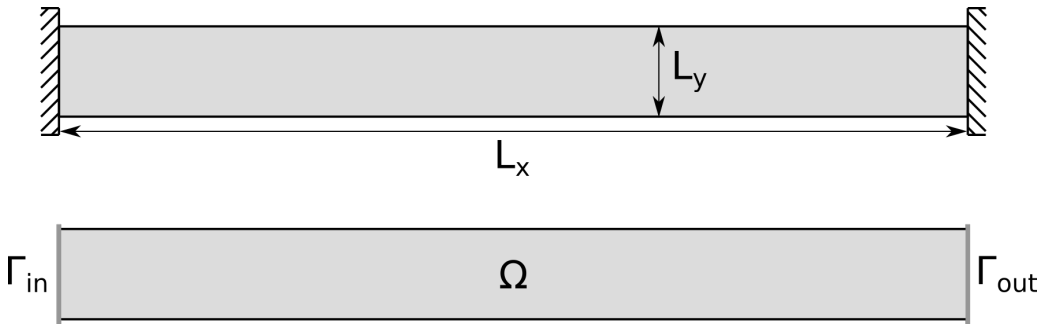

Figure 1 – Clamped-clamped beam

Two materials are considered in the optimization, a stiff material with $E_1 = 210$ GPa, $\nu_1 = 0.3$ and $\rho_1 = 7800$ kg/m^3; and a flexible material with $E_2 = 21$ GPa, $\nu_2 = 0.3$ and $\rho_2 = 780$ kg/m^3. The imposed volume fraction for the optimized structure is 60% of stiff material and 40% of flexible material. The connectivity is imposed for the stiff material, that is, there must be a continuous path between Γ_{in} and Γ_{out} composed only by the stiff material. Elements composed by the flexible material are treated as void elements in the virtual heat problem, with a nearly zero thermal conductivity.

The domain is discretized in a mesh of 600×30 square elements, and four-node bilinear elements in plane-stress state are used in the FEA.

The beam is optimized for an operating frequency of 17 kHz. Starting from a structure completely composed by the stiff material, the solutions from Figure 2 are obtained. The first one is obtained when no connectivity constraint is imposed, and the second one is obtained when a minimal thickness of 20 mm is imposed through VFM. Elements in black correspond to the stiff material, and elements in gray correspond to the flexible material.

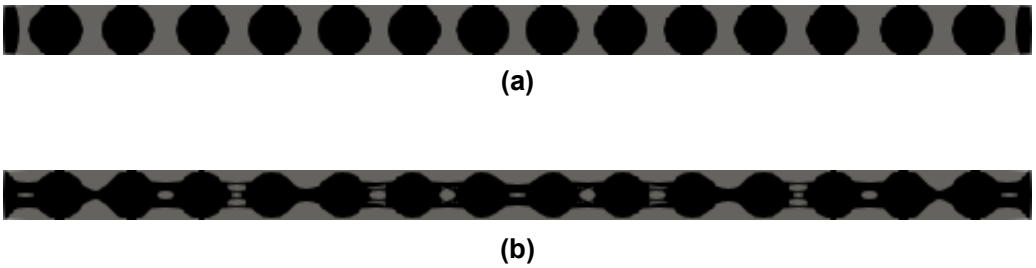

Figure 2 – Optimized clamped-clamped beams (f_0 = 17 kHz), (a) without VFM and (b) with VFM

The minimal connection thickness has been maintained in the constrained case. When optimizing the structure with the connectivity constraint, the algorithm redistributes some of the material to form efficient connections between each circular component of the unconstrained solution.

Their frequency responses are presented in Figure 3. It can be noted that the disconnected structure is very efficient, with a frequency gap of 14.2 kHz. Evidently, the inclusion of the connectivity constraint reduces the performance of the optimized structure. Nonetheless, the natural frequencies around the operating value have successfully been separated, while keeping the desired connectivity. A gap of 6.3 kHz has been obtained for the constrained problem.

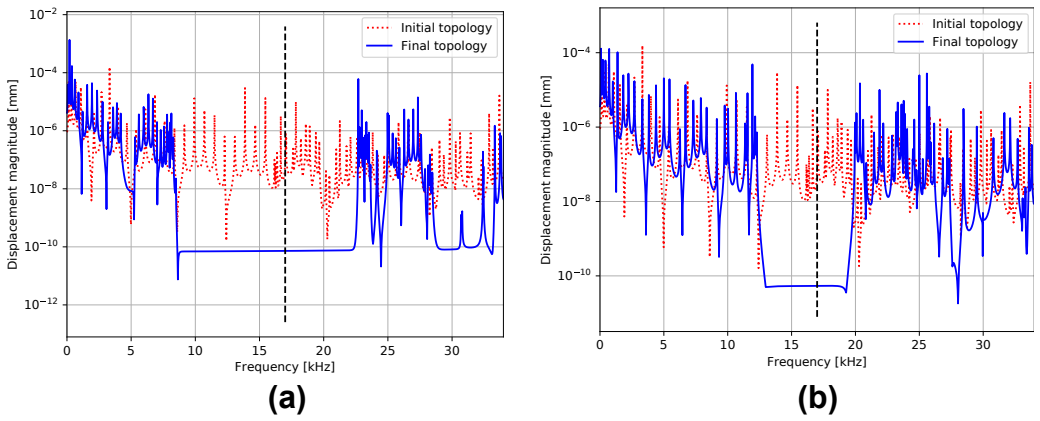

Figure 3 – Frequency responses of the optimized clamped-clamped beams (f_0 = 17 kHz) (a) without VFM and (b) with VFM

Ring Structure

In this section, a ring structure is considered, as illustrated in Figure 4. The dimensions of the ring-shaped design domain are $R_1 = 270$ mm and $R_2 = 370$ mm.

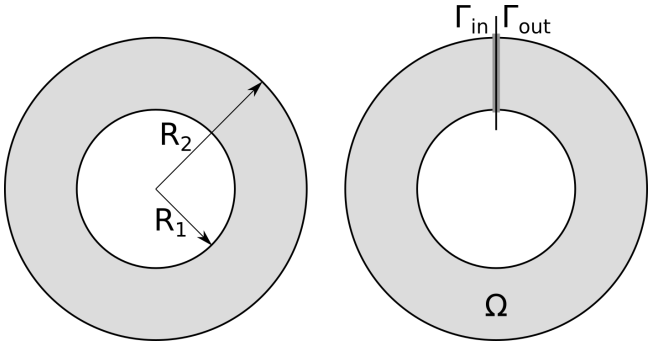

Figure 4 – Ring structure

The VFM is used to impose that the structure corresponds to a proper ring, so any arbitrary section must be connected to itself through a path going around the ring. So Γ_{in} and Γ_{out} overlap. In order to obtain the desired behavior, the nodes corresponding to these overlapping regions are duplicated in the virtual heat problem. So Γ_{in} and Γ_{out} are only connected through paths going around the ring, as illustrated in Figure 5, in which a perspective view of the domain is bent so the duplicated nodes can be identified.

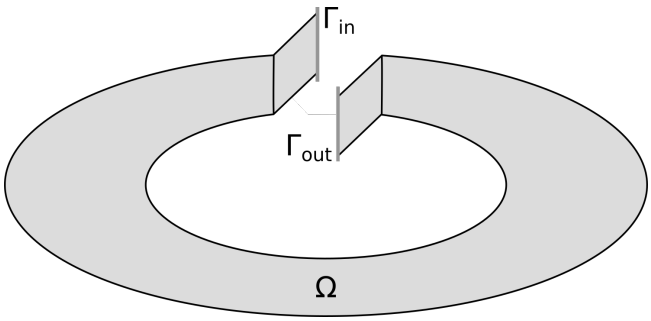

Figure 5 – Ring structure with duplicated section to apply the VFM

Besides the overlapping of the regions to be connected, this problem presents another particularity. If the initial topology is axisymmetric, then all elements that are at the same distance from the center will have the same sensitivity value. Therefore, if the initial topology corresponds to a structure completely composed of the stiff material, a whole sub-ring would be removed (turned into flexible material) in the first iteration, disconnecting the structure over the radial direction.

Connectivity could be imposed between the inner and outer edges of the ring, however, this would not solve the problem. Since the sub-ring is removed in a single iteration, the VFM would not be capable of identifying any critical elements to inhibit their removal. Alternatively, the number of altered elements could be reduced in order to avoid instant disconnections, however, there is no sensible way to choose which from these equivalent elements should be altered and which should not.

This problem is solved by including perturbations on the initial topology in order to remove its axisymmetry. Although some bias is included by this procedure, results show that it has little influence on the optimization process. In this work, four holes of diameter $D = 30$ mm are included in the initial topology, as presented in Figure 6.

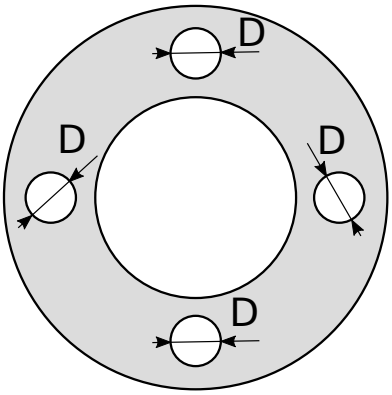

Figure 6 – Initial topology for the ring structure

The domain is discretized in a mesh of 600×30 trapezoidal elements, and four-node bilinear elements in plane-stress state are used in the FEA.

The ring is first optimized for an operating frequency of 17 kHz. The solutions from Figure 7 are obtained. The first one is obtained when no connectivity constraint is imposed, and the second one is obtained when a minimal thickness of 20 mm is imposed through VFM. Elements in black correspond to the stiff material, and elements in gray correspond to the flexible material.

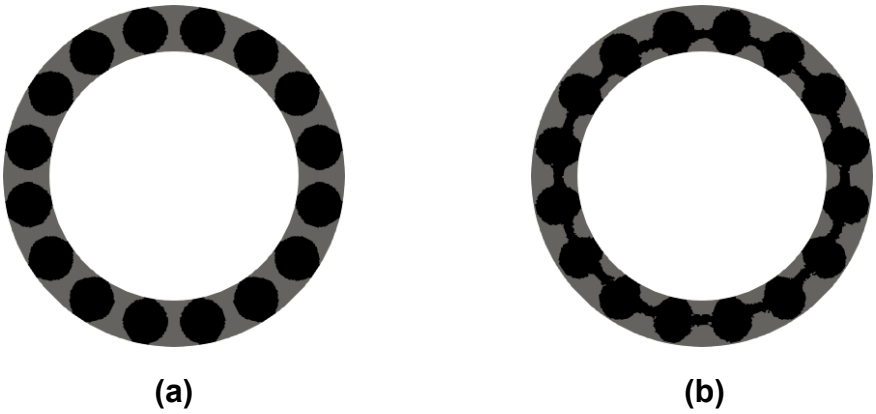

Figure 7 – Optimized ring structures (f_0 = 17 kHz), (a) without VFM and (b) with VFM

It can be noted that this result is very similar to the one obtained for the clamped-clamped beam. This is not unexpected, periodic results are often obtained for the clamped-clamped beam when high operating frequencies are considered, and a ring structure with a large enough inner radius should have similar behavior than a periodic clamped-clamped beam.

As in the clamped-clamped beam case, the minimal connection thickness has been maintained in the constrained case. When optimizing the structure with the connectivity constraint, the algorithm redistributes some of the material to form efficient connections between each circular component of the unconstrained solution. In Figure 8, the VFM activation value of each element is shown for the optimized structure, elements in blue are unconstrained, and elements in red are prevented from being removed (turned into flexible material).

Figure 9 presents how the natural frequencies of the structure are altered throughout the optimization process. In the first iterations, two groups of frequencies are established, the ones above the operating frequency and the ones below it. Then, each group is clustered, and each cluster gradually moves away from the operating frequency value.

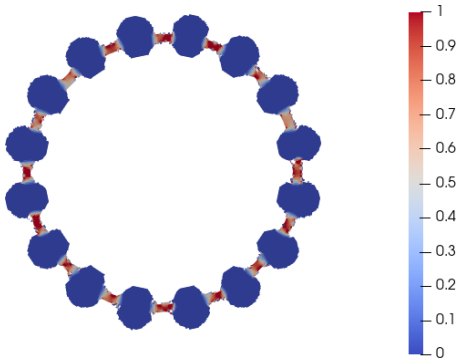

Figure 8 – VFM activation for the optimized ring structure (f_0 = 17 kHz)

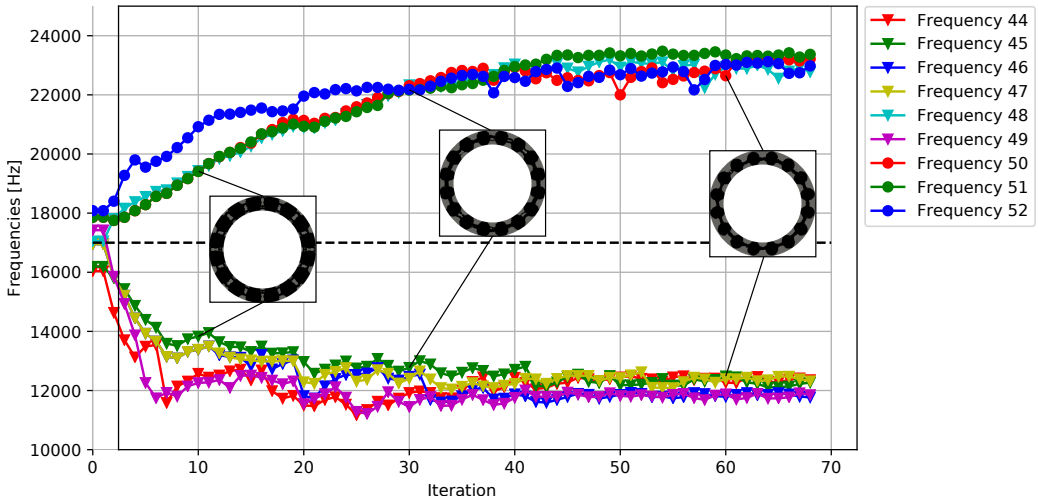

Figure 9 – Natural frequencies throughout the optimization process (f_0 = 17 kHz)

The corresponding frequency responses are presented in Figure 10. The obtained frequency gaps are 14.7 kHz for the disconnected structure and 9.9 kHz for the connected one.

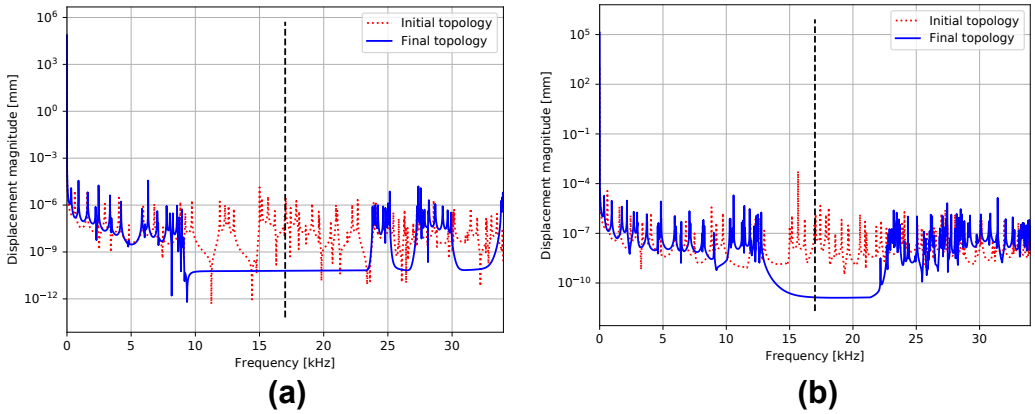

Figure 10 – Frequency responses of the optimized ring structures (f_0 = 17 kHz) (a) without VFM and (b) with VFM

By performing this optimization for an operating frequency of 12 kHz, the solutions from Figure 11 are obtained. And by performing it for an operating frequency of 5 kHz, the solutions from Figure 12 are obtained.

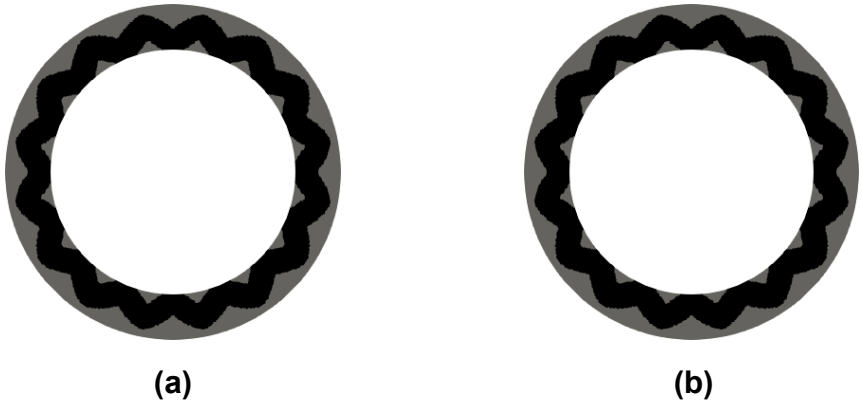

Figure 11 – Optimized ring structures (f_0 = 12 kHz), (a) without VFM and (b) with VFM

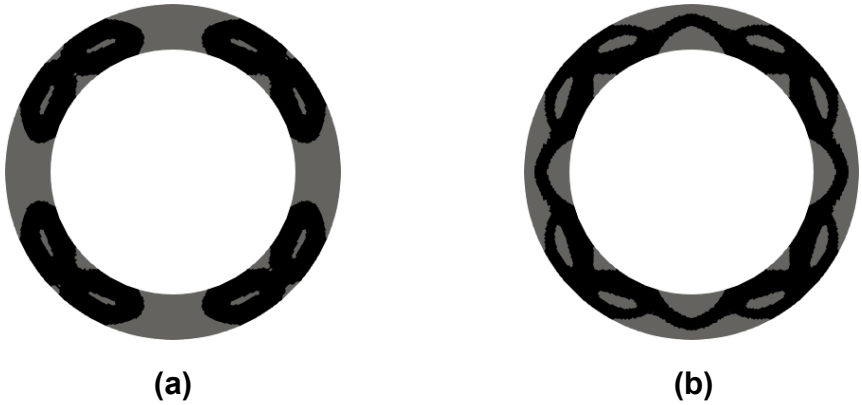

Figure 12 – Optimized ring structures (f_0 = 5 kHz), (a) without VFM and (b) with VFM

For $f_0 = 12$ kHz, the unconstrained optimization already results in a connected structure. The obtained frequency gap is 3.9 kHz. As expected, if it is not advantageous for optimizing the objective function, the optimization process does not produce disconnected topologies. In this case, the VFM is never fully activated, so it has little influence on the result.

On the other hand, for $f_0 = 5$ kHz, the unconstrained optimized structure is once again disconnected. As before, when the VFM constraint is included, the algorithm redistributes some of the material to form efficient connections between each component of the unconstrained solution. The frequency separation for the disconnected topology is 3.0 kHz, and 2,2 kHz for the connected one.

CONCLUSIONS

The formulation of the topology optimization problem for separating natural frequencies has been presented, together with the BESO algorithm coupled with the VFM, in order to impose connectivity constraints.

Results have been generated for a clamped-clamped beam with two materials, considering a high operating frequency of 17 kHz. It has been shown that the inclusion of the VFM constraint guarantees the specified minimal connection thickness while still producing an efficient structure, with a frequency gap of 6.3 kHz around the operating frequency.

Then, the method has been applied to a ring structure, for different operating frequencies. In order to properly use the VFM in this case, the domain has to be divided, with duplicated nodes over the dividing section. The virtual heat problem is stated so that the dividing section is connected to itself, through a path going around the ring. Moreover, initial topologies that are not axisymmetric have to be considered in order to avoid degenerated results. By taking these two extra considerations into account, the BESO-VFM optimization has successfully produced efficient structures respecting the imposed minimal connection thickness.

The following frequency gaps have been obtained for the connected structures: 9.9 kHz, for $f_0 = 17$ kHz; 3.9 kHz, for

$f_0 = 12$ kHz; and 2,2 kHz for $f_0 = 5$ kHz. For the case with $f_0 = 12$ kHz, the result of the unconstrained optimization already corresponds to a connected structure, so the VFM activation has little effect on the optimization process.

This work has illustrated a particular application of the VFM for imposing connectivity constraints in topology optimization problems. It has been shown that the VFM can be applied in domains with different geometries and particularities with simple adaptations. For the considered cases, efficient results, with little bias from the VFM constraint, have been obtained. In future steps, VFM may be applied to three dimensional structures, and to problems with different classes of objective functions.

ACKNOWLEDGMENTS

This work was supported by FAPESP (São Paulo Research Foundation, grant numbers 2013/08293-7, 2019/19237-7 and 2019/05393-7).

REFERENCES

Bendsøe, M. P., and Kikuchi, N., 1988, "Generating optimal topologies in structural design using a homogenization method", Computer methods in applied mechanics and engineering, Vol. 71, No. 2, pp. 197-224.

Ewins, D. J., 2009, "Modal testing: theory, practice and application", John Wiley & Sons.

Jensen, J. S., and Pedersen, N. L., 2006, "On maximal eigenfrequency separation in two-material structures: the 1D and 2D scalar cases", Journal of Sound and Vibration, Vol. 289, No. 4-5, pp. 967-986.

Liu, S., Li, Q., Chen, W., Tong, L., and Cheng, G., 2015, "An identification method for enclosed voids restriction in manufacturability design for additive manufacturing structures", Frontiers of Mechanical Engineering, Vol. 10, No. 2, pp. 126-137.

Lopes, H. N., Mahfoud, J., and Pavanello, R., 2021, "High natural frequency gap topology optimization of bi-material elastic structures and band gap analysis", Structural and Multidisciplinary Optimization, Vol. 63, No. 5, pp. 2325-2340.

Lopes, H. N., Cunha, D. C., Pavanello, R., and Mahfoud, J., 2022, "Numerical and experimental investigation on topology optimization of an elongated dynamic system", Mechanical Systems and Signal Processing, Vol. 165.

Ma, Z. D., Cheng, H. C., and Kikuchi, N., 1994, "Structural design for obtaining desired eigenfrequencies by using the topology and shape optimization method", Computing Systems in Engineering, Vol. 5, No. 1, pp. 77-89.

Olhoff, N., Niu, B., and Cheng, G., 2012. "Optimum design of band-gap beam structures", International Journal of Solids and Structures, Vol. 49, No. 22, pp. 3158-3169.

Pedersen, N. L., 2000, "Maximization of eigenvalues using topology optimization", Structural and multidisciplinary optimization, Vol. 20, No. 1, pp. 2-11.

Pereira, R. L., Lopes, H. N., and Pavanello, R., 2022, "Topology optimization of acoustic systems with a multiconstrained BESO approach", Finite Elements in Analysis and Design, Vol. 201.

Querin, O. M., Steven, G. P., and Xie, Y. M. , 1998, "Evolutionary structural optimisation (ESO) using a bidirectional algorithm", Engineering computations.

Seyranian, A. P., Lund, E., and Olhoff, N., 1994, "Multiple eigenvalues in structural optimization problems", Structural optimization, Vol. 8, No. 4, pp. 207-227.

Xie, Y. M., and Steven, G. P., 1996, "Evolutionary structural optimization for dynamic problems", Computers & Structures, Vol. 58, No. 6, pp. 1067-1073.

Yang, X. Y., Xie, Y. M., Steven, G. P., and Querin, O. M., 1999, "Topology optimization for frequencies using an evolutionary method", Journal of Structural Engineering, Vol. 125, No. 12, pp. 1432-1438.

Zhao, C., Steven, G. P., and Xie, Y. M., 1997, "Evolutionary natural frequency optimization of two-dimensional structures with additional non-structural lumped masses", Engineering Computations.

Zhou, M., and Rozvany, G. I. N., 1991, "The COC algorithm, Part II: Topological, geometrical and generalized shape optimization", Computer methods in applied mechanics and engineering, Vol. 89, No. 1-3, pp. 309-336.

Zuo, Z. H., Xie, Y. M., and Huang, X., 2010. "An improved bi-directional evolutionary topology optimization method for frequencies", International Journal of Structural Stability and Dynamics, Vol. 10, No. 1, pp. 55-75.

RESPONSIBILITY NOTICE

The authors are the only parties responsible for the printed material included in this paper.